Tutors

Dra. Marina Inés Giannotti
Centro de Investigación Biomédica en Red
Institut de Bioenginyeria de Catalunya

Dr. Francesc Mas
Departament de Ciència de Materials i
Química Física

Grau de Química

Treball Final de Grau

Stretching of weak polyelectrolytes at the single-molecule level.
Estirament de polielectròlits febles a nivell d'una sola molècula.

Silvia Sodric Hidalgo

June 2019

Universitat de Barcelona

B:KC Barcelona Knowledge Campus
Campus d'Excel·lència Internacional

Imagination is more important than knowledge.
Knowledge is limited. Imagination encircles the world.

Albert Einstein

I would like to express my very great appreciation to Dra. Marina Inés Giannotti and Dr. Francesc Mas, my research supervisors, for their patient guidance, enthusiastic encouragement and valuable suggestions during the planning and development of this project. My grateful thanks are also extended to Dr. Sergio Madurga and Pablo Blanco for their dedication in the follow-up to this project. And specially, for having introduced me to the world of computational chemistry.

I would also like to thank all my family and friends for the support they have given me on this long road to achieve this project.

REPORT

CONTENTS

1. SUMMARY 3
2. RESUM 5
3. INTRODUCTION 7
3.1. Hyaluronan description 7
3.1.1. HA physical properties and its applications 8
3.1.2. HA conformations and viscosity under specific conditions 8
3.2. AFM-SMFS 10
3.2.1. Principles of AFM-SMFS 10
3.2.2. Theoretical ideal models 12
4. OBJECTIVES 14
5. EXPERIMENTAL SECTION 14
5.1. Materials 14
5.2. Preparation of buffers, substrates and HA solutions 15
5.2.1. Buffers preparation 15
5.2.2. Substrates preparation 15
5.2.3. HA solutions preparation 15
5.3. Summary of the experimental conditions 16
5.4. Data acquisition 17
6. THEORETICAL BACKGROUND 18
6.1. A minimal description of the site binding model of stretched polyelectrolytes 18
6.2. Monte Carlo simulations 21
7. RESULTS AND DISCUSSION 24
7.1. Experimental results 24
7.1.1. Desorption events 24
7.1.2. Stretching events 27
7.2. Simulation results 30

7.2.1. HA titration 30
7.2.2. Effect of the pH-value in the force-extension curves 31
7.3. A comparison of experimental and simulation results 35
8. CONCLUSIONS 37
9. REFERENCES 39
10. ACRONYMS 41
APPENDICES 43
Appendix 1: Calibration of AFM cantilever 44
Appendix 2: Histograms of desorption force 45
Appendix 3: Force extension curves 49

1. SUMMARY

The goal of this project consists in the study of the mechanical response of weak polyelectrolytes at the single-molecule level in order to evaluate the interplay between Charge Regulation (CR) and mechanical stretching. Specifically, the chosen weak polyelectrolyte has been hyaluronic acid HA, also called hyaluronan. The mechanical response during stretching of weak polyelectrolytes is an area still under study. Weak polyelectrolytes can modulate their charge in response of external stimuli (such as pH changes, ionic strength or by electrostatic interactions with other charged species) and, for this reason, it is expected that their mechanical properties will also change. The present work was carried out by single molecule force spectroscopy (SMFS) using an atomic force microscope (AFM) under liquid environmental control and Monte Carlo based computational simulations in order to investigate the influence of pH changes and salt concentration on the behavior of the elasticity of HA single chains.

For the nanomechanical AFM-SMFS characterization of single HA (physically adsorbed onto glass, mica and silicon substrate), an AFM tip was used to pick up and stretch the single chains. Upon separation of the tip and the substrate, the macromolecule attached onto the substrate is first uncoiled and then stretched or desorbed. At larger extensions, the force increases strongly with the extension in a nonlinear manner until pulling force becomes at one point so large that the molecule detaches from the tip. In this case, when the macromolecule is strongly attached to the AFM tip and substrate, stretching (also called pulling) events were observed which has a characteristic spike in the force curve profile. On the other hand, if the macromolecule is weakly attached to the substrate and the tip is retracted, the macromolecule is being peeled away. In this new situation, desorption events were observed with various force plateaus. These results were obtained in pH 4 and 5.7, and pH 5.7 with 0.1 M NaCl solution, where macromolecules are in different ionized degrees. Force spectroscopy clearly reflects the influence of the different environments. The obtained force extension curves suggest that the measured force needed to stretch a single chain up to certain extension decrease at pH 5.7 compared to pH 4 and no differences were observed comparing pH 5.7 with and without added salt. In the case of

desorption events, the plateau force increased from pH 4 to pH 5.7. This suggests that the affinity between macromolecule and the surface is better in the solvent with the higher pH-value.

Finally, the experimental data recorded were compared using mechano-statistical theories (specifically Worm-Like Chain model, WLC) and simulation Monte Carlo (MC) computational methods. With this aim, we used a minimal model that captures the fundamental aspects present in the stretching of a weak linear polyelectrolyte: bond stretching, bond bending and proton binding. Mechanical stretching was performed using Grand Canonical Monte Carlo (GCMC) simulations at different pH and ionic strength values. The force-extension curves show the effect of pH and ionic strength on polyelectrolyte stretching. Simultaneously, these simulations also provide conformational (persistent length l_p and chain elongation L_z) and protonation properties (degree of protonation θ and the effective acidity constant pKa). It can be observed that at large force regimes, the force-extension curves were approximately independent of the pH and the ionic strength I. Finally, the comparison between the experimental and computational force-extensions curves suggest that both follow the same general trend but in different force regimes.

Keywords: polyelectrolyte, stretching, desorption, force spectroscopy, atomic force microscope, Monte Carlo simulation.

2. RESUM

L'objectiu principal d'aquest projecte consisteix en l'estudi de les respostes mecàniques de polielectròlits febles a nivell d'una sola molècula per tal d'avaluar la relació entre la regulació de la càrrega i l'estirament mecànic. El polielectròlit amb el que es farà l'estudi és l'àcid hialurònic HA, un polímer natural. La resposta mecànica durant l'estirament de polielectròlits febles és una àrea encara poc explorada. La càrrega dels polielectròlits febles canvia en funció del medi (p.e. canvis en el pH, temperatura, força iònica o per interacció amb altres espècies carregades) i, per aquesta raó, es esperable que les seves propietats mecàniques també canviïn. Aquest estudi s'ha portat a terme mitjançant espectroscòpia de forces atòmiques (AFM), en un medi líquid controlat i amb simulacions computacionals pel mètode Monte Carlo, per tal d'investigar la influència dels canvis de pH i de força iònica en el comportament elàstic de les cadenes de HA.

Per a la caracterització nanomecànica AFM-SMFS a nivell d'una sola molècula de HA (físicament adsorbida sobre un substrat de vidre, mica o silici), es va utilitzar una punta AFM per agafar i estirar les cadenes de manera individual. Després de la separació de la punta i del substrat, la macromolècula lligada al substrat es desenrotlla i després s'estira o s'arrossega sobre la superfície. A extensions més grans, la força augmenta fortament amb l'extensió de manera no lineal fins que la força de tracció es tan gran que la molècula s'acaba desprenent de la punta. En aquest cas, quan la macromolècula està fortament lligada a la punta de l'AFM i al substrat, s'observen esdeveniments d'estirament els quals tenen un pic característic al perfil de la corba de força. D'altra banda, si la macromolècula està unida feblement al substrat i la punta s'allunya, en comptes d'estirar-se entre dos punts prèviament fixats s'arrossega per sobre de la superfície. En aquesta cas, es van observar esdeveniments de desorció amb diferents altiplans de força. Els resultats obtinguts van ser a pH 4 i 5.7, i pH 5.7 amb una solució de NaCl 0.1 M, on les macromolècules es troben amb graus de ionització diferents. L'espectroscòpia de forces atòmiques reflecteix clarament la influència dels diferents entorns. Les corbes de força-extensió obtingudes suggereixen que la força mesurada necessària per estirar una sola cadena a una certa extensió disminueix a pH 5.7 i no s'observen diferències comparant pH 5.7 amb i sense sal afegida. En el cas dels esdeveniments de desorció, l'altiplà de la força va augmentar de pH 4 a

pH 5.7. Això suggereix que l'afinitat entre la macromolècula i la superfície és millor com més alt sigui el pH.

Finalment, les dades experimentals registrades es van comparar mitjançant teories mecano-estadístiques (en concret amb *Worm-Like Chain model*, WLC). També es va comparar amb mètodes computacionals de simulació Monte Carlo (MC). Amb aquest objectiu, s'ha proposat un model simplificat que capta els aspectes fonamentals presents en l'estirament d'un polielectròlit lineal feble: estirament d'enllaços, flexió d'enllaços i unió de protons. L'estirament mecànic es va realitzar mitjançant simulacions de *Grand Canonical Monte Carlo* (GCMC) a diferents valors de pH i de força iònica. Les corbes de força-extensió mostren l'efecte del pH i de la força iònica en l'estirament d'un polielectròlit. Simultàniament, aquestes simulacions també proporcionen informació sobre les propietats conformacionals (longitud de persistència l_p i allargament de cadena L_z), així com de les propietats de protonació (grau de protonació θ i la constant d'acidesa efectiva pKa). Com es podia esperar, a règims de força alts les corbes de força-extensió són gairebé independents del pH i de la força iònica. Finalment, la comparació entre les corbes de força-extensió experimentals i computacionals suggereixen que ambdues segueixen la mateixa tendència general, però en règims de força diferents.

Paraules clau: polielectròlit, estirament, desorció, espectroscòpia de forces, microscòpia de forces atòmiques, simulació Monte Carlo.

3. INTRODUCTION

In nature, most of the relevant processes involve mechanical movement at the single molecule level. In addition, the macroscopic properties of polymeric materials are directly related to the primary chemical composition, structure, conformation and interactions at the molecular level. Nanomechanical studies of single polymer chains contribute to the comprehension of fundamental aspects concerning the structural, mechanical, and binding properties of macromolecules. Understanding their elastic behavior is an essential issue in both life science and materials science.

3.1. HYALURONAN DESCRIPTION

Polyelectrolytes (PEs) are long chain molecules consisting of many identical subunits that acquire an electric charge upon dissolution in water. They play an important role in industrial as well as in biological processes. For instance, polypeptide, DNA and glycosaminoglycans are polyelectrolytes. Hyaluronan (also called hyaluronic acid, HA) is a glycosaminoglycan that is found primarily in the extracellular matrix of some vertebrate connective tissues and pericellular matrix, but it has also been shown to occur intracellular as well as in some bacterial capsules, thus contributing significantly to many basic cellular processes [1].

HA is a linear, unbranched polysaccharide composed of identical disaccharide units containing glucuronic acid and N-acetylglucosamine, that are linked via altering β-1,4 and β-1,3 glycosidic bonds (Figure 1). Each disaccharide, which is 1 nm long, carries one chargeable carboxylic group. For polymeric HA, the intrinsic pKa is approximately 4.2 [2], which implies that HA is negatively charged at physiological pH. HA has a molecular weight of typically a few million Dalton, corresponding to contour lengths of several micrometers [3].

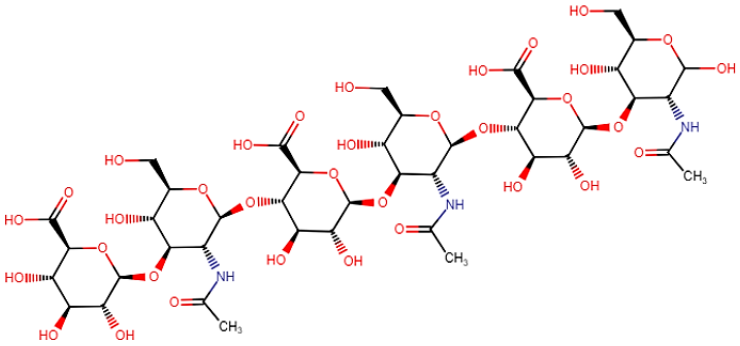

Figure 1. Structure of three monomers of HA polyelectrolyte.

3.1.1. HA physical properties and its applications

Nowadays, there is an increasing number of possibilities for its applications in the biomedical field that lie in the exploitation of its specific biological properties. This is a result of hyaluronan directly communicating with proteins and cells present in tissues. However, most of its functions are based on its physical properties, such as hydration, viscosity, and space filling. Some of the biological functions of HA include maintance of elastovisity of liquid connective tissues such as joint synovial fluid and eye vitreous, control of tissue hydration and water transport, and supramolecular assembly of proteoglycans in the extracellular matrix. The HA conformation in the extracellular matrix, under normal physiological conditions, is generally believed to exist as crowded random coil. When HA is under specific pathological conditions, its structure can be quite different [4]. The extensive repertoire of biological functions of HA suggest the existence of a correspondingly binding interactions. It is likely that the conformation is affected by the local environment.

3.1.2. HA conformations and viscosity under specific conditions

The conformations of HA in the dried and hydrated state has been meticulously determined by IR spectroscopy on HA films. It is well-know that HA adopts a helical conformation in the solid state [4] and all of these structures are stabilized by hydrogen bonds linking adjacent sugars residues across both glycosidics linkages. It has been demonstrated that HA shows different structures depending on the state: in dried state HA has an intramolecular hydrogen-bonded

organization but in hydrated state, HA adopts a hydrogen-bonded intermolecular structure where a water wires bridge the chains [1].

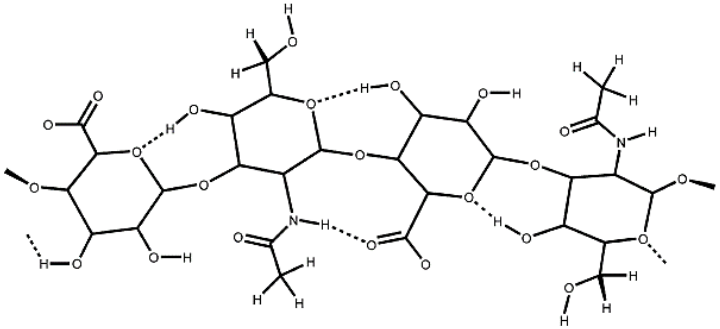

Figure 2. Local conformation of a fragment of HA with a representation of interchain hydrogen bonds that exist in the dried state [1].

Additionally, there are some studies that show the effect of certain environmental variables on HA solution such as the temperature or ionic strength dependence. The temperature dependence of the intrinsic viscosity of HA has been investigated by Cleland [5] and Fouissac et al. [6] the temperature range was 25-60ºC and they observed a decrease of persistence length, leading to a decrease on intrinsic viscosity. A temperature dependence of molecular elasticity at the single molecular level has also been demonstrated [1].

When carboxyl groups are protonated, the intramolecular electrostatic repulsion decrease, reducing the intrinsic viscosity in the absence of added salt. On the other hand, at low ionic strength, intramolecular and intermolecular electrostatic repulsion increases. Therefore, the measured intrinsic viscosity also increases in a manner expected for a flexible polyelectrolyte [4]. There are also several reports still unverified of changes in intrinsic viscosity of HA with pH changes. For instance, Barret and Harrinton [7] reported a pH-dependent transition. It has been proved to use phosphate buffers in the pH range 6.0-8.5 at an ionic strength of 0.1 M. They observed a dramatic drop in zero shear intrinsic viscosity as pH decreased from 7.5 to 7.0. This reduced viscosity to zero was quite high opening the possibly that a small change in bulk viscosity due to aggregation could result in an erroneous estimation of the intrinsic viscosity. This was re-examined by Balazs et al. [8] and they didn't observe any changes in intrinsic viscosity between pH 6 and 8 under the same conditions.

3.2. AFM-SMFS

Atomic force microscopy (AFM) was invented in 1986 as a high-resolution imaging technique giving topographical information by means of tracking contact forces between an AFM tip and a sample surface. This technique has been applied in a variety of research fields, including physics, chemistry, biology and biomedical sciences. For instance, AFM can visualize atoms and molecules and chemical bonds when imaged at low temperatures, as well as conformations of polymers in their various environments.

A decade after the invention of the AFM, Gaub and coworkers showed that AFM can also be used to manipulate and to extend single polymer molecules [9]. It allows the measurement of intramolecular and intermolecular forces ranging from the pN regime to the nN regime. The technique also allows the determination of molecular conformation by detecting molecular and supramolecular structures in biological macromolecules as well as in synthetic polymer systems [10]. The AFM-SMFS technique has some advantages such as combining the possibility of locating and proving single molecules under environmentally controlled conditions. In the present work, AFM-SMFS was used under conditions of variable and controlled pH and ionic strength.

3.2.1. Principles of AFM-SMFS

The principles of AFM-SMFS technique are schematically shown in Figure 3a. In short, the core components of an AFM device include: a flexible cantilever, featuring a tip at its free end; a piezoelectric translator that moves the sample stage or the cantilever depending on the design; an optical deflection system composed of a laser, a segmented photodiode, and a signal processing unit, which records the changes in cantilever deflection.

For the force spectroscopy analysis, the macromolecular chains can be physically or chemically adsorbed onto a solid substrate on the piezoelectric tube, which is able to perform precise movements in the z direction.

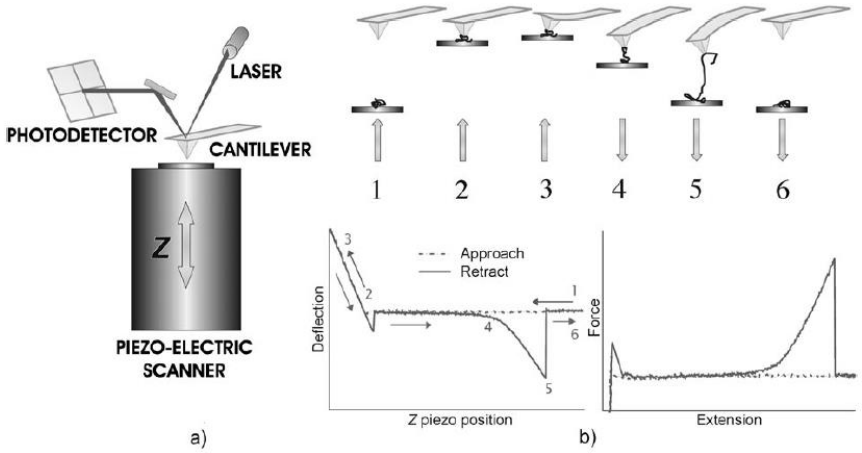

Figure 3. A schematic of the AFM and the force measurement. (a) Schematic illustration of the fundamental components of an AFM device with working principles. (b) Schematic illustration of a single-molecule deflection–displacement (piezo position) and force-extension curves [11].

Figure 3b schematically shows the movement of the piezoelectric positioner and the cantilever deflection during an approach–retract cycle. A force experiment begins with positioning of the functionalized cantilever a few hundreds of nanometers above the sample surface (Figure 3b, position 1). Then, the cantilever is moved towards the sample surface and makes contact with the sample surface (approach; Figure 3b, position 2). The deflection signal is at constant value corresponding to zero force until the tip contacts the surface. While tip and sample are in contact, the cantilever is further pushed toward the sample surface (positive change of the deflection/force signal), and the macromolecules on the substrate can adsorb onto the tip (Figure 3b, position 3). Then, the cantilever starts to move back to its initial position. After the course of backward movement of the cantilever (retraction), the linking macromolecule is first uncoiled (Figure 3b, position 4), and stretched if a specific interaction has been formed between the macromolecule attached on the surface and the tip. Accordingly, the cantilever bends further downwards (Figure 3b, position 5). In this part, a negative deflection is registered. As the chain is further stretched, the weakest point of the structure breaks due to a gradual increase of the tension applied. In other words, the macromolecule can desorb either from the surface or from the tip. Finally, the cantilever returns to its initial position (Figure 3b, position 6) [12].

The deflection-displacement profile registered, which describes the elasticity of a macromolecule, can be converted in force-extension curves by using some equations. The piezo position (z_0) is converted into the distance between the tip and the surface (z, called extension) using Equation 1:

$$z = z_0 - 1/S * D \quad (1)$$

Where D is the cantilever deflection and S the slope (voltage/length) of the recorded bending of the cantilever upon contacting the surface (linear part of the curve). Then, the deflection of the cantilever can be converted into force (F) by the Hooke's law depicted in Equation 2:

$$F = -k_S * (z - z_0) \quad (2)$$

Here, k_S is the spring constant of the cantilever and the minus sign of the Equation 2 is necessary to transform the negative deflection into a positive force signal, as shown in Figure 3b which depicts the force (F) against the extension (z).

3.2.2. Theoretical ideal models

The force-extension data recorded during stretching experiments are usually compared with the predictions of single chain elasticity models. Situations in which the polymers interact with the surface via weak potentials comparable with thermal energy have been well studied by experimental, theoretical, and simulation techniques. When a single polymer chain is stretched, two kinds of restoring forces occur. Brownian molecular motion causes a permanent fluctuation of the molecule, if a single chain adopts a random-coil conformation. Extension of the molecule leads to a reduction in the number of possible conformations, which causes a loss of conformational entropy. Hence, entropic forces dominate at short extensions (low stretching forces). On the other hand, large elongations relative to the chain contour length (its length at maximum physically possible extension, L_c) between the tip and the substrate lead to stresses in the molecular backbone. Bonds become stretched and deformed in the pulling direction, and the corresponding enthalpic elasticity is recorded in addition to the entropic forces [11].

In parallel to the experimental work, to describe the entropic elasticity of a polymer chain several theoretical approaches have been developed, differing in the detail of description of the macromolecular structure. In the first one, called Freely Jointed Chain (FJC) model, the polymer chain is represented at the Coarse-Grained level by a set of rigid links joined with fully random

orientation [13]. Although it is able to account for the stretching properties of a wide variety of synthetic polymers with different structures and solvents, this model was shown to present clear deviations from the elastic response of many other macromolecules of interest, such as double stranded DNA (ds-DNA). In other words, this model is thus a good approximation for small elongations (small applied forces) of the molecule. Aiming at overcoming these limitations, Marko and Siglia modeled the polymer as a Wormlike Chain (WLC) which, assuming exponential decaying correlations between chain segments, accounted for the capability of the chain to deform on short length scales [14, 15]. The resulting high force regime matched very well to a variety of polymers for which electrostatic interactions can be neglected.

As an alternative to these Coarse-Graining approaches, theoretical methods based on first principles, which account for the detailed atomistic structure of the macromolecular backbone have also been proposed. In these studies, *ab initio* calculations are firstly performed in order to detect the more stable conformational states of the interacting monomers at different elongations of the bonds. Once the structural microscopic information is available, the necessary thermal averages are performed by using Monte Carlo (MC) simulation. The resulting scheme has been successful in reproducing the experimental force-extension curves of several polymers. In particular, the stretching behavior of HA. There are methods which only account for short range interactions and can't thus be applied to charged macromolecules for which the long range coulombic forces can't be neglected. However, the presence of self-avoiding electrostatic forces produces new elastic regimes, which strongly deviate from the ideal, non-interacting, FJC and WLC models.

In the case of weak polyelectrolytes, the charge is in general a dynamical and fluctuating variable. This fact leads to the phenomenon of Charge Regulation (CR), defined as the capability of weak polyelectrolytes to modulate their ionization state as a response to some physicochemical perturbation. CR is ubiquitous in a wide range of processes of biological, environmental and technological interest. A few examples are the stability of colloidal systems and nanoparticle coating, receptor-ligand interactions in biochemical systems, and protein–protein and protein-surface interactions [16]. The paradigmatic mechanism for CR is the binding of protons and other small ions present in the backward medium. An outline of the used methodology is reported in section 6.

4. OBJECTIVES

The main objective of this project is the study of the mechanical response of a single HA chain during its stretching using the AFM-SMFS technique. In order to evaluate the charge regulation of the polymer chains with their elastic properties, the experiments will be carried out in different environments, with variations of pH and ionic strengths. On the other hand, the desorption forces at the single molecule level in different environments will also be analyzed. Finally, the force-extension profiles will be compared to mechano-statistical theories. In this case, it will be used the Wormlike Chain model with different values of persistent length (l_p) to compare the exponential fit of the experimental force-extension curves profiles. In parallel, a minimal model of the weak linear polyelectrolyte will be performed, and then analyzed by means of simulations in the Grand Canonical Monte Carlo (GCMC) computational method. Finally, a comparison between the experimental force-extension curves with the simulation will be carried out.

5. EXPERIMENTAL SECTION

5.1. MATERIALS

Hyaluronic acid (HA) sodium salt (also called sodium hyaluronate) from *Streptococcus equi* used for the experiments was purchased from Sigma-Aldrich. This HA has a molar weight about 120.000-350.000 g. mol^{-1} and has a storage temperature of -20ºC. For the liquid environmental control different buffers were used, which includes acetic acid and disodium hydrogen phosphate. Then, sodium chloride was used for ionic strength control. These salts were also purchased from Sigma Aldrich.

AFM force spectroscopy experiments were performed with an MFP-3D atomic force microscope (Asylum Research) using V-shaped Si_3N_4 cantilevers with Si tips and nominal spring constants of 0.06 $N.m^{-1}$ (Sharp Nitride Lever SNL, Bruker AFM Probes). The cantilever spring constants were individually calibrated using the equipartition theorem (thermal noise routine) [17], after measuring the sensitivity S ($V.m^{-1}$). All the experiments were performed under liquid conditions, using the corresponding buffer solution.

5.2. PREPARATION OF BUFFERS, SUBSTRATES, HA SOLUTIONS

5.2.1. Buffers preparation

In the first step, acetate buffers with two different pH-values (4 and 5.7) were prepared (pKa-value of acetic acid 4.76). The buffers were prepared in MilliQ water with a concentration of 0.05 M and an ionic strength due to the buffer of 0.045 M for the buffer with pH 5.7 and of 0.008 M for the buffer of pH 4. Then, each buffer was passed through a 0.22 µm pore size filter. In addition, acetate buffers with the same pH but with a concentration of 0.1 M NaCl were prepared, thus increasing the ionic strength to 0.145 M for the buffer with pH 5.7 and 0.108 for the buffer with pH 4. Finally, a phosphate buffered saline (PBS) with a pH of 8 and a concentration of 0.05 M (ionic strength 0.143 M) was prepared and then filtered.

5.2.2. Substrates preparation

- Glass: a) small 1 cm x 1 cm glass squares were cut out of glass slides using a diamond tip. The substrates were immersed in prepared piranha solution (mixture of 70% H_2SO_4 and 30% H_2O_2), rinsed thoroughly with ultrapure water and gently blow-dried with a stream of N_2. Then, the surfaces were stored in glass vials, previously rinsed in the same way, which contained a solution of HA in acetate buffer at pH 5.7, with a concentration of 0.5 $\mu g.ml^{-1}$. b) Alternatively, the glass substrates were cleaned using organic solvents. First, they were rinsed with ethanol and then with chloroform. Between these steps, the surfaces were dried under a stream of N_2. Then, they were stored in miliQ water and overnight incubated in a HA solution of 1.18 $\mu g.ml^{-1}$ at pH 5.7.

- Mica: these surfaces didn't need any previous treatment. The freshly cleaved mica surface was incubated in the HA solution at pH 5.7 for 15 minutes.

- Silicon: the rest of surfaces that were used for the experiments were silicon, which they were cut using the diamond pen into 1 cm x 1 cm squares. Afterwards, different treatments were assessed: rinsing with piranha, organic solvents and incubated with different times and concentrations of HA solution.

5.2.3. HA solutions preparation

Different HA solutions were prepared for the experiments. First one was the most concentrated: 200 $\mu g.ml^{-1}$ in ultrapure water. The second had 0.5 $\mu g.ml^{-1}$ HA concentration in

acetate buffer with a pH of 5.7. Finally, the last one had a concentration of 1.18 μg.ml^{-1}, also in the same buffer. These solutions were stored at 4ºC in vials rinsed with piranha.

5.3. SUMMARY OF THE EXPERIMENTAL CONDITIONS

To perform the force-extension curves by using an AFM, different environmental conditions were chosen, such as pH and ionic strength. Different HA concentration and surfaces were tested to find the optimal conditions, as shown below:

-System 1: the surface used was glass surface treated with piranha solution that makes the surface more hydrophilic, allowing the polymer to adhere better to the glass surface. The concentration of HA was 0.5 μg.ml^{-1} in acetate buffer with pH 5.7 and a time incubation of HA solution with the surfaces of 24 hours. Before the experiment, the surface was dried with stream of N_2 and rinsed two times with buffer. At each environmental change, pH 4 and 5.7, the surface was cleaned with the corresponding buffer.

-System 2: surface of glass treated with organic solvents was used under environmental control with acetate buffer, only at pH 5.7 acetate buffer. This treatment with chloroform and ethanol makes the surfaces less hydrophilic than piranha. Incubation time of the surfaces was approximately two days, with HA solution of 1.18 mg.ml^{-1} in pH 5.7. Then, before the experiment, glass surface was dried with N_2 and rinsed with acetate buffer at pH 5.7.

-System 3: in this case, mica was tested. Mica has a negatively charged surface, like HA chains. No events at pH 5.7 were observed, due to a weak interaction with this surface.

-System 4: silicon surfaces was prepared with piranha solution, stored under water and then incubated with HA solution of 1.18 mg.ml^{-1} in pH 5.7 for 15 minutes. Before using these surfaces for the experiment, they were rinsed with buffer at pH 5.7 and then dried with a stream of N_2. A force curves without adhesion or desorption and some curves with stretching events were obtained at pH 5.7. Thereby, silicon surfaces would be used in the rest of systems.

-System 5: silicon surfaces treated with organic solvents were used with HA concentration of 1.18 μg ml^{-1} in pH 5.7 and the incubation time were about 48 hours. Then, pH 4 and 5.7 was used for liquid environment. Moreover, in most of the force-extension curves, desorption events were obtained.

-System 6: silicon surfaces treated with piranha solution were used with a new prepared HA solution of 0.5 μg.ml^{-1} at pH 5.7 and an overnight incubation. With these prepared surfaces, force

curves were obtained at pH 4 and 5.7 acetate buffer. With the same surfaces, an acetate buffers with 0.1 M of NaCl were used in both pH-values. Incubation time was only 15 minutes.

-System 7: Silicon surfaces treated with piranha solution were used. The HA concentration was 0.5 μg ml^{-1} at pH 5.7 and an overnight incubation. With these prepared surfaces, force curves were obtained with pH 4 due to acetate buffer, pH 4 with 0.1 M of NaCl and finally at pH 8 due to PBS. At each environment change, surface was cleaned with the corresponding buffer. Nonetheless, in force curves obtained with PBS did not appeared any type of event.

5.4. DATA ACQUISITION

After calibration of the AFM cantilever depicted in Appendix 1, force spectroscopy measurements are acquired by using the detailed procedure described below:

1. Record numerous force-distance curves at each experimental condition. We used the following values for the experimental parameters: trigger point (maximum applied force when approaching; 500 pN), tip speed of 1 $\mu m.s^{-1}$ and a force distance of 500 nm.
2. Note that trigger point is a user defined value that tells the piezo to switch directions even if the force (deflection) curve hasn't achieved the complete force (deflection) distance value. It is possible to maintain the trigger force for certain desired contact time (dwell), that can be varied to reach a successful event.
3. It is important to move within the XY plane between force curves to probe fresh regions and prevent surface degradation. Force curves can be acquired individually by single force or continuously. There is another continuous mode that is making force map, which shows the force curves in a previously established area of the surface.
4. Finally, continue collecting the data until a significant number of force-distance curves is reached.

6. THEORETICAL BACKGROUND

6.1. A MINIMAL DESCRIPTION OF THE SITE BINDING MODEL OF STRETCHED POLYELECTROLYTES

In this work, we will make use of a model, which, containing a minimum number of parameters, still captures the fundamental aspects present in the stretching of a flexible weak linear polyelectrolyte: bond stretching, bond bending and proton binding. The HA polyelectrolyte, outlined in Figure 1, can be considered a simplification of a previously proposed model for a linear HA polyelectrolyte.

Let us assume that the chain is symmetric (i.e. the chain has a plane of symmetry when it is completely elongated) and contains a deprotonating site every three chain positions. In Figure 4, inert and deprotonating sites are depicted in orange and red, respectively. A macromolecule where N is the number of bonds and M represents the number of monomers (Figure 4), one per protonating site, thus contains N = 4M + 1 bonds.

The protonation equilibria are treated using the Site Binding (SB) model [16, 18], for which the protonating sites can adopt two possible states: protonated (uncharged site) and deprotonated (charged side) due to carboxylic group present in red site. Within the SB approach, the ionization state of the macromolecule can be characterized by a set of variables $s = s_i, i = 1, \dots, M$, with values 0 (deprotonated) or 1 (protonated).

For simplicity, all electrostatic interactions are described by Debye-Hückel potential (long range interactions, LR), mediated by the solvent. Finally, we introduce the possibility of elastic bond stretching and bending.

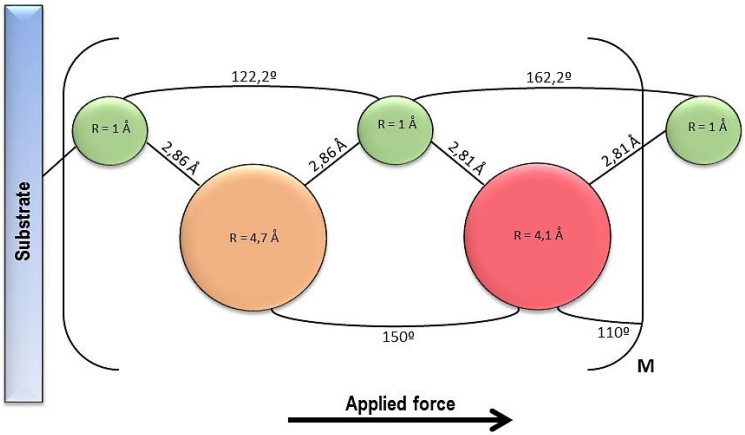

Figure 4. Outline of the proposed model for the weak polyelectrolyte. The monomers are represented as sites joined by flexible bonds with bending and stretching states and proton binding. Two kind of sites are considered: inert sites (green and orange) and deprotonating sites (red). The latter can adopt two possible states: protonated (uncharged site) or deprotonated (charged site), with protonation constant K_a. Only LR interactions mediated by the solvent and described by DH potential are considered. The angles, the bond distances and the radii of each "ball" represented in the present Coarse-Grained model have been measured by Avogadro program. Green sites represent the oxygens, orange sites are the sugars with an amide group and red sites with a carboxylic group from the HA polyelectrolyte.

Using SB model, which deals with ionization equilibria, the resulting free energy $\mathcal{F}$ can be expressed the sum of four contributions:

$$\mathcal{F} = W + \mathcal{F}_{length} + \mathcal{F}_{angle} + \mathcal{F}_{p} + \mathcal{F}_{LR} \quad (3)$$

Where the term

$$W = -\vec{F} \cdot \vec{r} \quad (4)$$

Represents the mechanical work exerted by the applied force $\vec{F}$, which is considered to act in the z-axis direction and r is the polyelectrolyte chain end-to-end vector. $\mathcal{F}_{\text{length}}$ and $\mathcal{F}_{\text{angle}}$ quantify the elastic deformation of the length and the angles of the *N* bonds, which can be important at large forces. In this work they are represented by the harmonic potentials:

$$\mathcal{F}_{length} = \sum_{j=1}^{N} \frac{k_{length,j}}{2} \left(l_j - l_{j,o}\right)^2 \quad (5)$$

$$\mathcal{F}_{angle} = \sum_{j=1}^{N-1} \frac{k_{angle,j}}{2} \left(\alpha_j - \alpha_{j,o}\right)^2 \quad (6)$$

Here l_j , α_j, $l_{j,o}$ and $\alpha_{j,o}$ represent, respectively, the length, the bending angle, the equilibrium length and the equilibrium bending angle of bond j. Finally, $k_{length,j}$ and $k_{angle,j}$ denote the bond stretching and bending force constants. Note the geometrical parameters and the force constants in the potentials (Equation 5 and 6) do not depend on the ionization state of the sites. At this level of description, this is a reasonable approximation which show only small variations in the bond lengths. On the other hand, the bond bending and bond stretching will be induced by the mechanical work at high enough forces, rather than by electrostatic repulsions. The term $\mathcal{F}_p(s)$ refers to the binding free energy, which can be expressed in terms of ionization state $s = \{s_i\}$:

$$\mathcal{F}_p(s)\cdot\frac{1}{ln10} = \sum_{i=1}^{M} \mu_i \, s_i \tag{7}$$

Where $\mu_i = pH - pKa_i = -\log(Ka_H)$ is the reduced chemical potential of the ionizable site *i*, which depends on the proton activity, a_H, and the intrinsic acidity pKa-values of the protonation constant of the site *i*, pKa_i.

Finally, the electrostatic interaction free energy has been considered as a Long Range (LR) $\mathcal{F}_{LR}$ contributions. These LR electrostatic interactions will be described by the Debye-Hückel potential (Equation 8). It is well established that LR interactions are chemically unspecific, mediated by the solvent, and can be reasonably approximated by a simple pair-interaction continuous force field.

$$\beta\mathcal{F}_{LR}(s) = \sum_{i=1}^{M}\sum_{j=i+1}^{M} \frac{l_B}{d_{ij}} \cdot e^{-\kappa d_{ij}} q_i q_j \tag{8}$$

Where d_{ij} is the distance between the sites i and j, $\kappa^{-1}(nm) = 0{,}304\sqrt{I(M)}$ is the Debye length for water at 298.15 K with ionic strength I and $\beta = (k_B T)^{-1}$. l_B~ 0,7 nm is the Bjerrum length in water at 298.15 K referring to the distance at which two elemental charges are separated so that the interaction energy is equal to the thermal energy. This value comes from the following equation, which depends only on the medium and temperature:

$$l_B = \frac{1}{4\pi\varepsilon_o\varepsilon_r}\frac{e^2}{k_B T} \tag{9}$$

To summarize, the model presented involves the following assumptions:

1. The SB model is used to describe the protonation equilibria on the same foot.
2. The molecule has one protonating site every three inert groups. As shown in Fig 4.

3. LR interactions are described by the DH potential, which account for screening effects so that co- and counter-ions intervene only in an effective way. Only excluded volume effects induced by electrostatics are considered.
4. The parameters involved in the model are equilibrium length and equilibrium angles of the bonds (l_0 and α_0) and constant forces for the bending and bond stretching (k_{length} and k_{angle}), which are considered the same for all the bonds and angles, *j* = 1, …, *N*. The control variables are the reduced chemical potential of the protonating sites $\mu = pH - pKa$ and the ionic strength (I), which are considered the same for all the protonating sites, i = 1,…, *M*.

6.2. MONTE CARLO SIMULATIONS

The proposed SB model is analyzed by means of simulations in the Grand Canonical Monte Carlo (GCMC), the pH-value is the control variable and it is kept constant along the computation. The GCMC code is a modification of the one previously to compute ionization properties of linear polyelectrolytes. In particular, it has been extended in order to include the effect of mechanical work [16]. As a result, bending and stretching of the bonds have also been implemented. The resulting program is rather general since it allows working with sites and bonds of different *pKa*-values, interaction energies, etc. Excluded volume effects can also be considered. Moreover, the code can deal with any arbitrary distribution of the sites along the chain, which is chosen by the user.

The Metropolis algorithm [19, 20] computed generates new states at constant pH in a chain with *M* = 50 ionizable sites, a number which is large enough to avoid end-effects and ensure the reproducibility of the intensive properties of the polymer, such as bond state probabilities or degree of protonation. An outline of the algorithm is depicted in Figure 5.

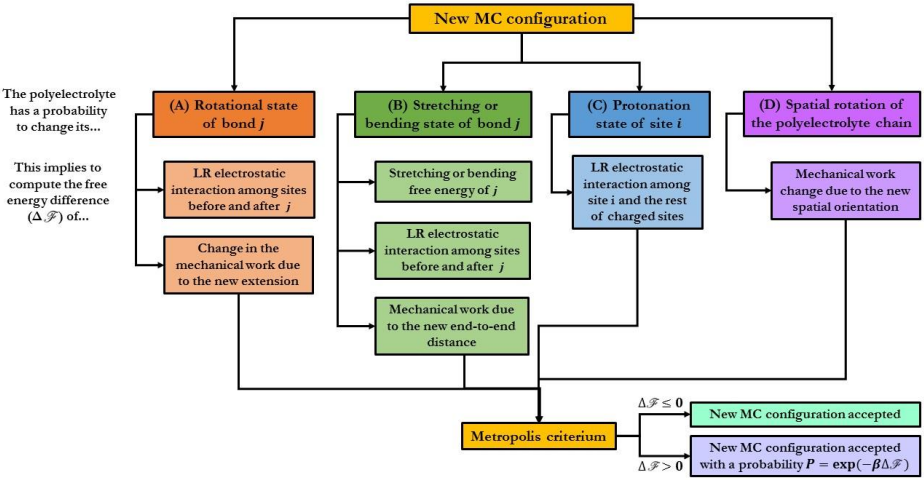

Figure 5. Metropolis algorithm of the GCMC simulation code. In each new MC simulation, the polyelectrolyte can change either (A) the rotational state of a bond, (B) the stretching or bending state of a bond, (C) the protonation state of a binding site and (D) the spatial orientation of the polyelectrolyte chain in laboratory coordinate frame with trial probabilities of 0.88, 0.1, 0.01 and 0.01 respectively.

In each new MC simulation, the polyelectrolyte can change either (A) the rotational state of a bond, (B) the stretching or bending state of a bond, (C) the protonation state of a binding site and (D) the spatial orientation of the polyelectrolyte chain in the laboratory reference frame, with trial probabilities 0.88, 0.1, 0.01 and 0.01 respectively. These values allow to obtain a good equilibration of the conformational structure for a given ionization state and are obtained using gran-canonical probability.

The average degree of protonation (θ) is computed as:

$$\theta = \frac{\langle M_p \rangle}{M} \tag{10}$$

Where $\langle M_p \rangle$ is the thermal average number of protonated sites. Is known that since the simulations are performed at constant pH-value, $\langle M_p \rangle$ is different in each new accepted configuration because is a fluctuating quantity. Additionally, another important quantity is the effective acidity constant (K_a), which is the inverse of the protonation constant (K_c) as shown in Equation 11. K_c provides information of the macromolecular sites for the protons. In other words, K_c depends on the charge of the macromolecule, which is different at each pH-value. Normally, the effective acidity constant K_a is described with the following acid-base equilibrium:

$$-A^- + H^+ \leftrightharpoons -\mathrm{AH}$$

Then, K_c can be written as:

$$pKa = logK_c = pH + \log(\frac{\theta}{1-\theta}) \quad (11)$$

The projection of the average in the extension of the polyelectrolyte chain (L_z) in the direction of the mechanical force, i.e. the z-axis, is obtained as:

$$L_z = \langle z_{M+1} - z_1 \rangle \quad (12)$$

Where z_i is z-coordinate of the site *i* in the laboratory coordinate frame. Then, the average square end-to-end distance $\langle r^2 \rangle$ considering the Freely Jointed Chain (FJC) model, is expressed as:

$$\langle r^2 \rangle_{FJC} = Ml_o \quad (13)$$

Where *M* and l_o are the number of ionisable sites and the equilibrium length of each monomer, respectively. In contrast, when FJC model is not considered, $\langle r^2 \rangle$ contains another parameter called the Kuhn length (l_k):

$$\langle r^2 \rangle = N_{fragments}\, l_k^2 = Ml_o l_k \quad (14)$$

Because of Equation 13, the Kuhn length becomes

$$l_k = \langle r^2 \rangle / Ml_0 \quad (15)$$

Finally, a very useful quantity for understanding the mechanism of macromolecular stretching is the persistent length, l_p. This parameter was introduced by Kratky and Porod [21, 22] as a direct measure of the average local conformation for a linear polymer chain. l_p reflects the sum of the average projections of all chain bonds $j \geq i$ on bond i in a specific direction described by a given segment. Below this length, the polymer is considered to be not correlated.

$$l_p / l_o = \sum_{j \geq i} \langle b_i \cdot b_j \rangle \quad (16)$$

Where b_i are unitary vectors pointing to the direction of the bonds. On the other hand, it can be demonstrated that persistent length is expressed as:

$$l_p = \frac{1}{2}(l_o + l_k) \quad (17)$$

Finally, for the ideal FJC model, the Kuhn length is equal to equilibrium length ($l_k = l_o$). As a result, persistent length is also the same ($l_k = l_o = l_p$).

7. RESULTS AND DISCUSSION

7.1. EXPERIMENTAL RESULTS

AFM-SMFS technique allows the characterization of single HA chains (physically adsorbed onto silicon surface) under environmentally controlled conditions. An AFM-tip was used to pick up and stretch the single macromolecules. The registered profile of the piezoelectric displacement-cantilever deflection was subsequently transformed into force-extension data corresponding to each single molecule stretching experiment.

In this section, the effect of the pH-value and the ionic strength on the force-extension curves will be discussed by AFM-SMFS. In the experimental data, both stretching and desorption events were observed. These events occur since the polymer is bridging the tip and the substrate, and when the tip is retracted, the polymer is progressively desorbed (Fig. 6a) or stretched (Fig. 6b).

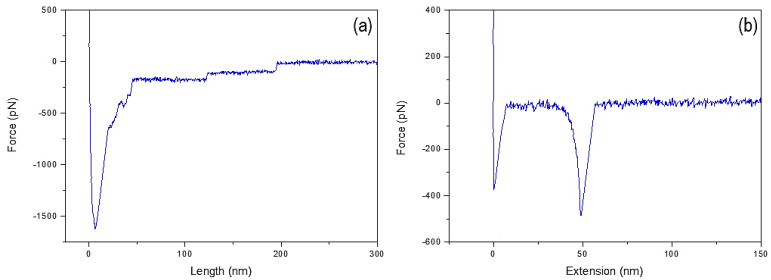

Figure 6. Single molecule force profiles on retraction. Two different types of observed events are (a) desorption (b) stretching or pulling.

7.1.1. Desorption events

Polymers weakly interacting with surfaces can be peeled from them, and this process leads to characteristic staircase-like force profiles. The desorption force represents a direct measure of the affinity between the polymer and the surface in the solvent in question. Desorption events are characterized by a constant plateau in the force curve. In this case, the molecule can be more weakly attached to the substrate or to the AFM-tip, and when the tip is retracted, the molecule is being desorbed, either by sliding or peeling. Note that single and several plateaus can be observed in a single cycle. Several plateaus would be characteristic for desorption events involving loops within individual molecules or originating from several polymer chains. Single HA chains were investigated by AFM adsorbed on glass, bare mica and silicon surface at pH 4, 5.7

in 0.05 M acetate buffer and pH 8 in 0.05 M PBS, where carboxylic groups are at different ionization degrees. A series of about 500 approach-retract force profiles were recorded. The individual force profiles vary substantially from one approach−retraction cycle to another. However, using determinate environments, specifically mica surface, glass surface with piranha treatment and PBS buffer at pH 8 in silicon, no events are recorded at all during a cycle.

HA was used to investigate the differences in the desorption behavior involving various environments. Histograms of the desorption forces for different surfaces and pH-values depicted in Appendix 2 reveal that their distribution is approximately Gaussian. The most probable desorption forces from force curves with two plateaus and its corresponding standard deviation has been measured by a Gaussian fit. Figure 7 shows examples of the desorption force curves of HA molecules adsorbed on different surfaces and a table summarizing the force values. We have been observed that the nature of the surface doesn't have a significantly influence in the magnitude of the desorption force. Desorption forces are similarly when silicon surface is used. Instead, desorption force in the second plateau decreases for glass surface.

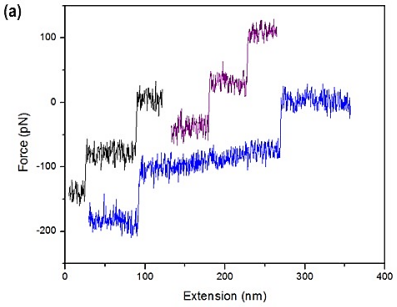

(b) pH 5.7	Desorption force 1 (pN)	Desorption force 2 (pN)
Silicon (organic solvents)	74.51 ± 7.06	157.84 ± 3.75
Silicon (piranha)	80.45 ± 5.82	153.06 ± 6.72
Glass	77.32 ± 7.90	137.00 ± 7.96

Figure 7. (a) Single molecule force profiles on retraction for HA polyelectrolyte on glass surface (black), silicon surface cleaned with organic solvents (blue) and cleaned with piranha (violet) at pH 5.7. (b) Most probable desorption forces and the corresponding standard deviation.

Figure 8 summarizes desorption forces at pH 4 of HA chains adsorbed on silicon with different previous treatments. In Figure 8a, one observes that desorption forces are practically the same. The values of average desorption forces and its standard deviation are depicted in Table 8b. The fact of not observing significant differences between different surfaces possibly due to the chain desorbing from the AFM-tip instead of the surface or both. For this reason, desorption force seems to be independent of the surface.

(a)

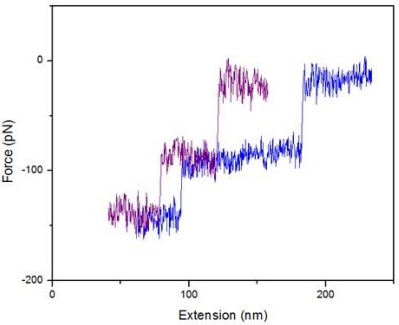

(b) pH 4	Desorption force 1 (pN)	Desorption force 2 (pN)
Silicon (piranha)	66.96 ± 4.97	129.84 ± 10.64
Silicon (organic solvents)	70.78 ± 6.35	127.47 ± 8.70

Figure 8. (a) Single molecule force profiles on retraction for HA polyelectrolyte on silicon surface cleaned with organic solvents (violet) and cleaned with piranha (blue) at pH-value 4. (b) Most probable desorption forces and the corresponding standard deviation.

Figure 9 displays the desorption force at pH 4 and 5.7 with a controlled salt concentration. Different pH-values was found to have substantial effect on the observed desorption forces. Figure 9a shows a typical force curves on retraction in both pH-values and Figure 9b shows force curves with added salt. The most probable desorption forces and its standard deviation are shown in Table 9c. It can be observed a decreasing of the desorption force when pH decreases. In other words, there is a greater interaction between single HA chains and surface when pH is 5.7. Finally, both pH-values in 0.1 M NaCl solution were compared. In this new situation, it has been observed that the desorption force becomes independent between both pH-values.

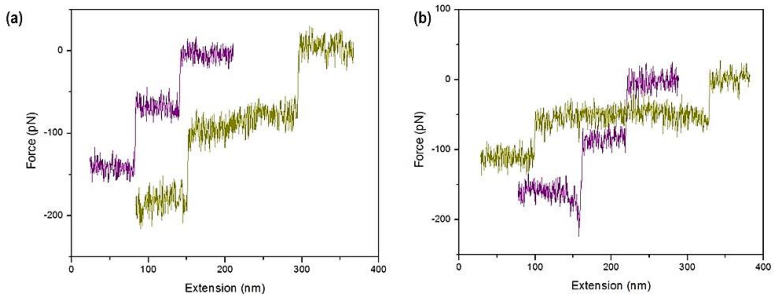

(c)	Desorption force 1 (pN)	Desorption force 2 (pN)
Silicon (pH 4)	66.96 ± 4.97	129.84 ± 10.64
Silicon (pH 5.7)	80.45 ± 5.82	153.06 ± 6.72
Silicon (pH 4, 0.1 M NaCl)	72.61 ± 7.85	137.89 ± 12.25
Silicon (pH 5.7, 0.1 M NaCl)	77.20 ± 9.63	152.19 ± 2.21

Figure 9. (a) Single molecule force profiles on retraction for HA polyelectrolyte on silicon surface cleaned with piranha at pH 4 (violet) and pH 5.7 (dark yellow) (b) in 0.1 M NaCl solution. (c) Most probable desorption forces and the corresponding standard deviation.

7.1.2. Stretching events

The elastic responses of HA chains were studied at three pH-values and with 0.1 M NaCl solution in some experiments, i.e., pH 5.7, pH 4 and pH 8. These pH-values were chosen due to the progressive increase of electrostatic repulsion observed in the polyelectrolyte when increasing pH. On the other hand, no events were observed using pH 8 and pH 4 in 0.1 M NaCl solution during AFM experiments. The force-extensions curves of single HA chains measured at pH 5.7, pH 4 and pH 5.7 in 0.1 M NaCl solution are depicted in Appendix 3. The extension was then normalized for each curve considering the extension at a defined force. The fact that the normalized curves superimpose well indicates that single HA molecules were stretched since the elastic properties scales linearly with the contour length [1]. Then, recorded data were plotted together for pH 4 and 5.7, and pH 5.7 and pH 5.7 in 0.1 M NaCl solution.

Therefore, with the intention of comparing the resulting force-extension data recorded during the stretching experiments at each environment, the force-extension data were normalized by the extension corresponding to a common force value (340 pN in this case). Afterwards, the normalized force-extension curves were plotted together as shown in Figure 10, which clearly shows the differences between each environment.

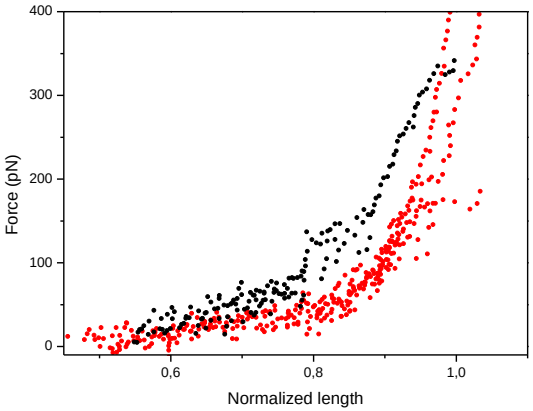

Figure 10. Superposition of the force-extension traces of individual HA molecules measured at pH 4 (black scatters) and 5.7 (red scatters) and then normalized to a common force value of 340 pN.

In order to evaluate the behavior of the single HA molecules at two pH-values, the results were compared to the WLC model. This theoretical model describes the polymer chain as a homogeneous string with a constant bending elasticity. It also treats the molecule as a continuous entity with persistent length l_p (the sum of the average projections of all chain segments in a specific direction). The contour length L_c of a polymer chain is its length at maximum physically possible extension and is equal to the product of the number of segments of the molecule and its length. The most commonly expression is the interpolation formula of Marko and Siggia [14, 15].

$$F(z) = \frac{K_B T}{l_p}\left[\frac{1}{4}\left(1 - \frac{z}{L_c}\right)^{-2} + \frac{z}{L_c} - \frac{1}{4}\right] \quad (18)$$

This model is effective to reproduce the force-extension (z) behavior for short extensions, but this approach is limited by the contour length, and fails for macromolecules under conditions of high stress. A simple exponential fit of the experimental force-extension curves was carried out to use as a guide, as depicted in Figure 11. We have also demonstrated that WLC model doesn't fit well at high force regimes (Figure 12).

Figure 11 clearly demonstrated that the measured force to stretch individual HA chains at a certain extension are different when both pH-values are compared. The structure of HA molecule is more folded at lower pH due to a decrease of electrostatic repulsion. Hence, the force to stretch an individual HA molecule results higher with a decrease of the pH, as is demonstrated by the superposition of the curves and its exponential fit at low force regime.

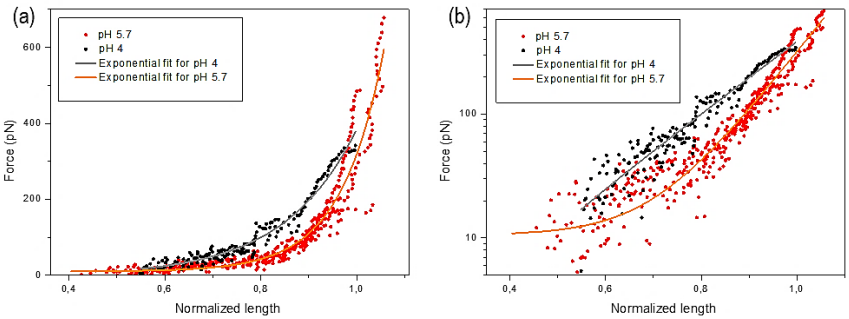

Figure 11. Superposition of the force-extension traces of individual HA chains plotted together at both pH-values with a simple exponential fitting. Force axis is represented in: (a) linear and (b) logarithmic scale.

Figure 12 shows the exponential fit in the experimental data and the WLC model with its deviation predictions from the experimental data. WLC model has been represented at different persistent length, which have been chosen from computational simulations (Figure 16). For this reason, the used persistent length range is 0.3, 0.5, 1, 1.5 and 3 nm. Although WLC model may fit the low forces regime, it's observed that its deviation from the experimental data increases when increasing force for every persistent length. This is consistent with the fact that WLC model is only valid for low values of applied force and it is also consistent with the simulation results.

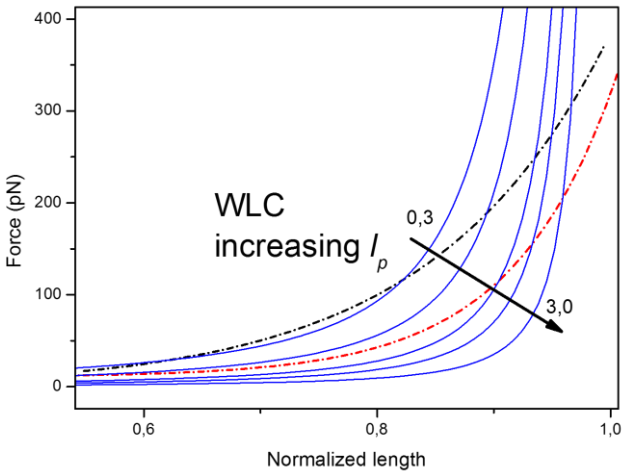

Figure 12. Exponential fitting of the force-extension traces of individual HA chains at both pH-values (red line for pH 5.7 and black line for pH 4). Then, superposition of WLC model (Equation 18) with a range of persistent length from 0.3 nm to 3 nm is performed (blue lines).

Finally, it has been plotted together force-extension curves at pH 5.7 with pH 5.7 in 0.1 M of NaCl solution (depicted in Figure 13) to analyze the effect of the ionic strength. Both experimental force curves were normalized by the extension at a common force value of 102 pN. The force to stretch single HA chains at a certain extension may be larger at high ionic strength than low ionic strength. Instead, there is no differences in the superposition of the normalized force-extension curves. This suggest that the stretching of HA chains seems independent with these values of ionic strength in this force regime.

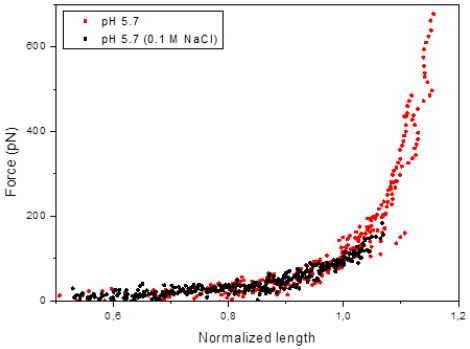

Figure 13. Superposition of the force-extension traces of individual HA chains plotted together at pH 5.7 (red scatters) and pH 5.7 with a higher ionic strength (black scatters).

7.2. SIMULATION RESULTS

In this section, the effect of pH-value and ionic strength on the force-extension curves will be discussed by simultaneously analyzing the dependence of conformational (chain elongation and persistent length) and protonation properties (degree of protonation and effective protonation constant). The intrinsic pKa is supposed to be equal to 4.2 [2] for all the protonating sites. Finally, the free energy (Equation 3) depends on the pH-value through the reduced chemical potential: $\mu = pH - pKa$, equal too for all the protonating sites.

7.2.1. HA titration

Since charge regulation is very important for the model, let us firstly analyze the behavior of the degree of protonation without any mechanical force applied, which will be useful in the discussion. Figure 14 displays the titration curves at four different ionic strengths (I): 1 M, 0.1 M, 0.01 M and 0.001 M, from top to bottom.

In Figure 14a it is observed that increasing the ionic strength results in a decrease of the degree protonation and it can be explained by a decrease of LR electrostatic repulsions. The effective acidity constant is depicted in Figure 14b. At high ionic strength pKa is constant with pH. Instead, as pH increases and lowering ionic strength, sites get ionized and the work needed to protonate an empty site increases due to electrostatic repulsion. This results in an increase of pK_a. At last, end-to-end distance $\langle r^2 \rangle$ and persistent length, l_p are shown in Figures 14c and 14d, respectively. In these figures, it can be observed that lowering the ionic strength and increasing the pH, HA chain becomes more stretched due to electrostatic repulsion, which leads end-to-end distance and persistent length larger.

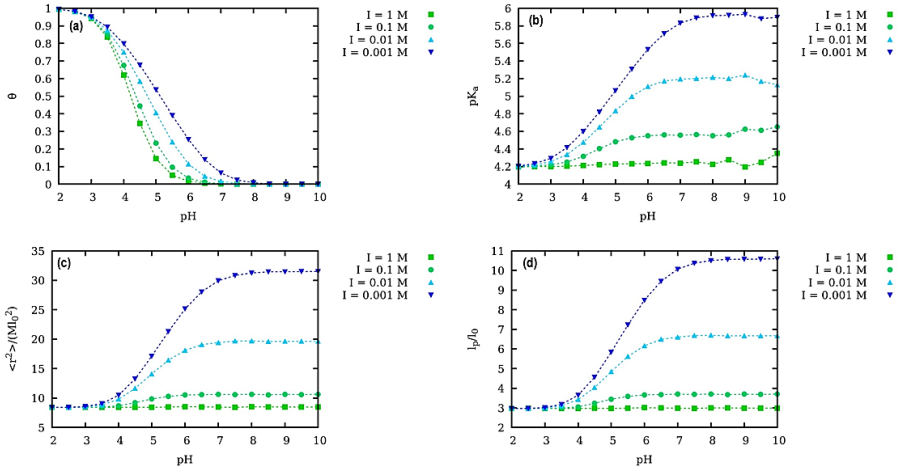

Figure 14. (a) Degree of protonation; (b) effective acidity constant; (c) end-to-end distance; and (d) persistent length *versus* pH for HA with pKa= 4.2 in absence of the pulling force. The chosen ionic strength are 1 M, 0.1 M, 0.01 M and 0.001 M. The $\langle r^2 \rangle$ is normalized with its expected value for an ideal model of a Freely Jointed Chain (FJC), which is Ml_o^2, where M = 50 is the number of monomers and l_o= 7.49 Å is the end-to-end equilibrium length for one monomer. The persistent length is normalized with the end-to-end equilibrium length for a monomer l_o.

7.2.2. Effect of pH-value in the force-extension curves

Force-extension curves are shown in this section. In Figure 15 applied force *versus* chain elongation is represented. Chain elongation is normalized to the contour length Ml_0. For Figure 15a, the chosen value for the ionic strength is 0.001 M, a small value for which the LR electrostatic interactions are maximized.

Figures 15b and 15c have the same pH and I values used in AFM experiments to recreate the experimental conditions (both pH with I due to the buffer solution, and both pH with a higher I). At high force regime is observed that the elongation of polyelectrolyte chain becomes approximately independent of pH and I because the chain gets very stretched. For Figures 15b and 15c, where the ionic strength is higher, it is observed differences between both pH-values at low force regime. Figure 15a shows clearly the effect of pH. In the low force regime, when the chain is more folded, it is observed that increasing the pH results in a decrease of force. It can be explained since at high pH the chain is more elongated because of an increase of the electrostatic repulsion. For this reason, less work is needed to stretch the chain at a certain extension.

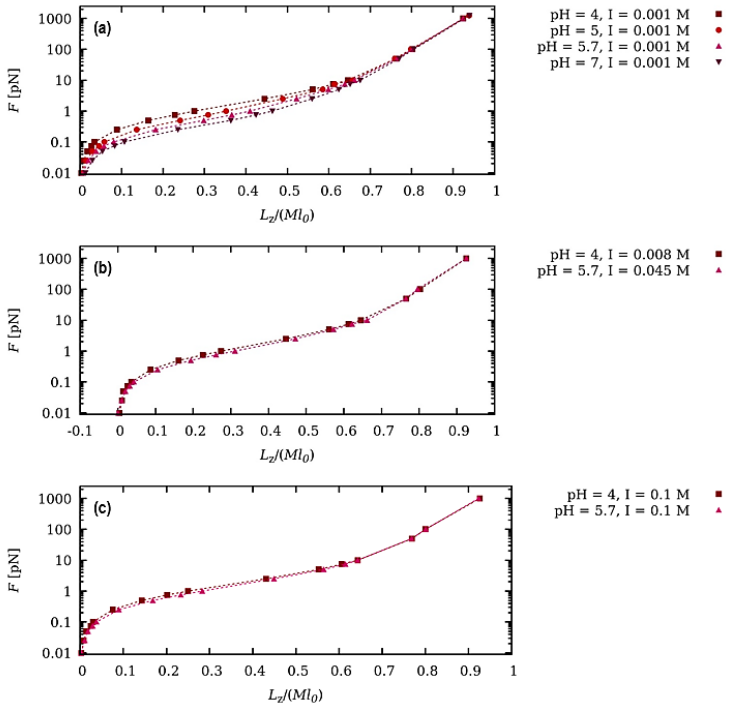

Figure 15. Applied force F *versus* chain elongation L_z (a) at constant ionic strength 0.001 M and pH-values 4, 5, 5.7 and 7; (b) at pH-values 4 and 5.7 and ionic strength 0.008 and 0.045 respectively; (c) at pH-values 4 and 5.7 and constant ionic strength 0.1 M.

In Figure 16 it can be analyzed the dependence of persistent length on force. At low force regime and low ionic strength (Figure 16a), when pH increases results in an increase of electrostatic repulsion, which increase the spatial correlation of neighboring bonds. In other words, most of the bonds are oriented in the same way in the space. For this reason, the persistent length increases. In contrast, the chain is more folded when pH decreases. Accordingly, the correlation between neighboring bonds and persistent length decreases. On the other hand, when the force is large enough to deform angles and length, an increase in the persistent length is observed independently of the ionic strength and pH because the chain starts to be significantly elongated. In this case, the spatial correlation is maximum since the bonds are oriented in the same way. Finally, in Figures 16b and 16c it can only be observed that the difference between pH-values are lower because the ionic strength is higher.

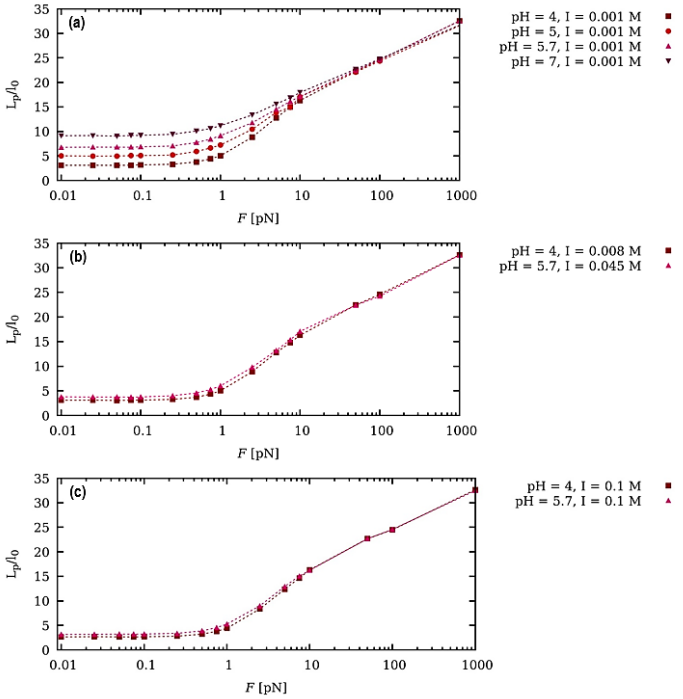

Figure 16. Persistent length l_p *versus* applied force F (a) at I strength 0.001 M and pH-values 4, 5, 5.7 and 7; (b) at pH-values 4 and 5.7 and ionic strength 0.008 and 0.045 respectively; (c) at pH-values 4 and 5.7 and I 0.1 M.

Finally, Figure 17 shows the dependence of the effective acidity constant pKa on the applied force. In the first case (Figure 17a), the value of ionic strength is lower than Figures 17b and 17c. In all cases, the effective pKa decreases with force since binding properties: the polyelectrolyte chain is on the average more elongated as F increases (high force regime). Hence, LR interactions decrease and the mean distance between sites increases, allowing more ionizable sites to be easily deprotonated. At last, in Figures 17b and 17c the ionic strength is larger. In this new situation, the decrease of the effective pKa with applied force would be weaker than at low ionic strength since there are less ionized sites in the polyelectrolyte chain.

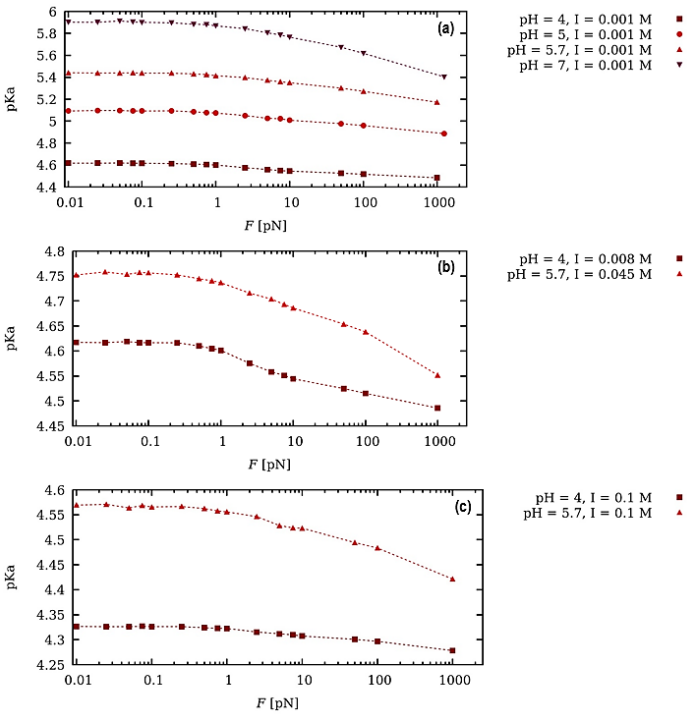

Figure 17. The effective acidity constant pKa *versus* applied force F (a) at constant ionic strength 0.001 M and pH-values 4, 5, 5.7 and 7; (b) at pH-values 4 and 5.7 and ionic strength 0.008 and 0.045 respectively; and (c) at pH-values 4 and 5.7 and constant ionic strength 0.1 M.

7.3. A COMPARISON OF EXPERIMENTAL AND SIMULATION RESULTS

In this section, simulation results and experimental data are compared for both pH-values and ionic strengths. As the force axis in simulation force curves are represented in a logarithmic scale, the experimental force-curves for each different environment were also represented in a logarithmic scale. Figure 18 summarizes these results. On the first hand, it is clearly observed that both simulation and experimental force curves follow the same general trend. The pulling force to stretch a single HA chain to certain extension is higher for the lowest pH value. In other words, under certain applied force, the HA molecule elongation is higher at pH 5.7 than at pH 4.

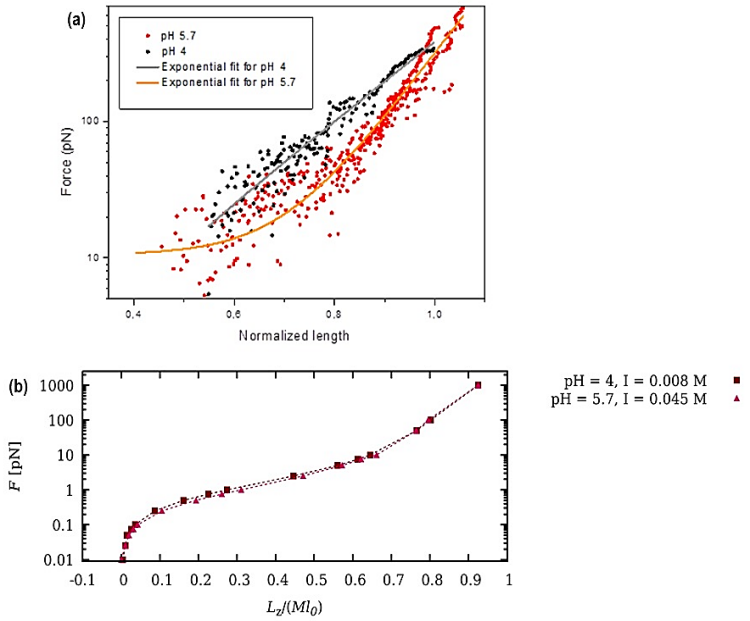

Figure 18. Comparison of both pH-values in: (a) Experimental force-extension traces of HA molecule with an exponential fitting. (b) Computational simulation of applied force *versus* chain elongation L_z

It is important to notice that, although the simulation and experimental results show a very good qualitative correlation, there is still work to be done to have a complete quantitative match. This is because the force regime where differences between each environment are observed is lower in the simulations than experimental force curves.

8. CONCLUSIONS

In the present work, the influence of Charge Regulation in the stretching properties of a weak linear polyelectrolyte was studied. With this aim, we proposed a model with a minimum number of parameters (proton binding, bond bending and bond stretching) which captures the fundamental aspects of a weak linear polyelectrolyte. It is based on the SB model which allows to study ionization properties. Bond stretching and bond binding are included by means of harmonic potential. LR electrostatic interactions are implemented using the mean field Debye-Hückel potential. The resulting scheme was used to perform Grand Canonical Monte Carlo (GCMC) simulations at different pH and ionic strength. In parallel, AFM-SMFS technique to evaluate the elasticity of single HA molecules under controlled liquid environment, including different pH and ionic strength, was carried out. Two kinds of single molecule events were observed and studied, namely desorption and stretching events. Finally, analyzing all these results we can conclude the following:

- Desorption forces do not depend strongly on the substrate, but a dependence with pH was observed. The desorption force at pH 5.7 is higher than pH 4. This means that the affinity of the HA molecule to the substrate or the AFM tip is greater at pH 5.7 than pH 4. These desorption forces were also analyzed with a higher ionic strength and both pH. In this situation, no dependence with pH was observed.
- Single HA chains stretching properties showed a dependence with the environment. The experimental force-extension curves clearly show that, under certain applied force, the HA molecule extension is higher at pH 5.7 than pH 4 due to the CR phenomena. The HA molecule is less negatively charged under pH 4 than pH 5.7. In other words, the HA molecule has different ionization degree depending on the pH. Hence, LR electrostatic interactions decreases at the lowest pH. As a result, a higher force is required to reach certain extension when the HA molecules are in a buffer of pH 4 (chains more folded) than pH 5.7 (chains more unfolded). At higher ionic strength and constant pH, the HA chains are more folded since a decrease of ionized sites. Although the force to stretch single HA chains at a certain

extension may be larger at high ionic strength, the comparison of force curves measured at pH 5.7 with and without added salt does not reveal any dependence.

- Although the WLC model may fit the low forces regime of the experimental curves, a deviation from the experimental data is clearly observed as the force increases, for every persistent length. This is consistent with the fact that WLC model is only valid for low values of applied force and it is also consistent with the simulation results
- As a general trend, two force regimes are found in the simulations of force-extension curves. The low force regime is the most interesting one since CR and spatial correlations are observed. It is also in this regime where pH and ionic strength I maximally influence the chain elongation L_z and persistent length l_p. These two parameters become approximately independent of the pH and I at large force regime where molecule is very unfolded. When the molecule is elongated, LR interactions decreases favoring the deprotonation of the sites. This results in a decrease of pKa which is larger at low I. It is also found that the influence of the pH (at a constant I) in L_z exhibits the same tendency that in experimental force curves. The reason is also explained by CR effect. On the other hand, at high pH, where LR interactions makes the chain more stretched, results in an increase of l_p (in low force regime) since a highly correlation of bonds.
- Both simulation and experimental results are clearly qualitatively comparable. The same trend of the extension under a certain applied force with respect to the environmental pH was observed. They cannot be quantitively compared since the force regime where differences in the elastic behavior of the polyelectrolyte are observed is much lower in the computational simulations than in the experimental data. The simple model of the polyelectrolyte here presented can be improve including the conformational free energy of the bonds for a given conformational state ($\mathcal{F}_{\text{rot}}$). On the other hand, the number of experimental stretching events achieved in pH 4 is lower than pH 5.7. For better comparison of the results more AFM experiments need to be carried out. Functionalization of the AFM tip and substrate could be another option to easily acquire stretching events.
- We would like to highlight that, even for the simple model of polyelectrolyte here presented, one finds rather rich physical-chemical behavior, which includes Charge Regulation. Up to our knowledge, this work is the first attempt to study the interplay between Charge Regulation and the mechanical stretching of a weak linear polyelectrolyte, by means of computational simulations and AFM-SMFS.

9. REFERENCES

[1] Giannotti, M. I.; Rinaudo, M.; Julius V. G. Force Spectroscopy oh Hyaluronan by Atomic Force Microscopy: From Hdrogen-Bonded Networks toward Single-Chain Behavior. Biomacromolecules, 2007**,** 8, 2648-2652.

[2] Cleland, L. R.; Wang, J. L.; Detweiler, D. M. Polyelectrolyte Properties of Sodium Hyaluronate. 2. Potentiometric Titration of Hyaluronic Acid. Macromolecules, 1982, 15, 386-395.

[3] Attili, S.; Borisov, V. O.; Richter, P. R. Films of end-graftet Hyaluronan are a prototype of a brush of a strongly charged, semiflexible polyelectrolyte with intrinsic exclude volume. Biomacromolecules, 2012**,** 13, 1466-1477.

[4] Cowman, K. M.; Matsuoka, S. Experimental Approaches to Hyaluronan Structure. Carbohydrate Research, 2005, 340, 791-809.

[5] Cleland, R. L. Effect of Temperature on the Limiting Viscosity number of Hyaluronic Acid and Chondroitin 4 Sulfate. Biopolymers. 1979, 18, 1821-1828.

[6] Fouissac, E.; Milas, M.; Rinaudo, M. Shear-rate. Concentration, molecular weight, and temperature viscosity dependences of Hyaluronate, a Wormlike Polyelectrolyte. Macromolecules, 1993, 26, 6945-6951.

[7] Barrett, T. W.; Harrington, R. E. Low velocity gradient flow birefringence and viscosity changes in Hyaluronate solutions as a function of pH. Biopolymers 1977, 16, 2167-2188.

[8] Balazs, E. A.; Cowman, M. K.; Briller, S. O.; Cleland, R. L.; On the limiting viscosity number of hyaluronate in potassium phosphate buffers between pH 6.5 and 8. Biopolymers, 1983, 22, 589-591.

[9] Radiom, M.; Kozhuharov, S.; Kong, P.; Giannontonio, M.; Mathieu, A.; Maroni, P.; Kilbinger, F. M.; Fromm, M. K.; Weder, C.; Borkovec, M. Quantitative Nano-Characterzation of Polymers using Atomic Force Microscopy. Chimia, 2017, 71, No. 4.

[10] Xi Zhang, X.; Liu, C.; Wang, Z. Force Spectroscopy of Polymers: Studying on Intramolecular and Intermolecular Interactions in Single Molecular Level. Polymer, 2018, 49, 3353-3361.

[11] Giannotti, M.I.; Julius, V. G. Interrogation of Single Synthetic Polymer Chains and Polysaccharides by AFM-Based Force Spectroscopy. ChemPhysChem, 2007, 8(16):2290–2307.

[12] Melissa, C. P.; Wouter, H. R.; Atomic Force Microscopy: An Introduction. (2018), pp: 243-258.

[13] Smith, S. B.; Bustamante. L. F. Direct mechanical measurements of the elasticity of single DNA molecules by using magnetic beads. Science, 1992, 258, 1122-1126.

[14] Bustamante, C.; Marko, J. F.; Siggia, E. D.; Smith, S. Entropic elasticity of lambda-phage DNA. Science, 1994, 265, 1599 –1600.

[15] Marko, J. F.; Siggia, E. D. Stretching DNA. Macromolecules, 1995, 28, 8759 –8770.

[16] Blanco, P., Madurga, S.; Mas, F.; Garcés, J. Effect of Charge Regulation and conformational equilibria in the stretching properties of weak polyelectrolytes. Submitted, 2019.

[17] Proksch, R.; Schaffer, T. E.; Cleveland, J. P.; Callahan, R. C.; Viani, M. B. Finite optical spot size and position corrections in thermal spring constant calibration. Nanotechnology, 2004, 15, 1344–1350.

[18] Garcés, J. L.; Madurga, S.; Borkovec, M. Coupling of Conformational and Ionization Equilibria In Linear Poly(ethylenamine): A Study Based On The Site Binding/Rotational Isomeric State (SBRIS) Model. Physical Chemistry Chemical Physics, 16(10):4626-4638, 2014.

[19] Ullner, M.; Jonsson, B.; A Monte Carlo Study of Titrating Polyelectrolytes in The Present Salt. Macromolecules, 29(20):6645-6655, 1996.

[20] Borkovec, M.; Jönsson, B.; Koper, G. J. M. J. Surface and Colloid Science, vol. 10. Plenum Press (Matigeric, E.; ed.) New York, USA, 2001.
[21] Porod G.; Monatsh. Zusammenhang zwischen mittlerem End-punktsabstand und Kettenlänge bei Fadenmolekülen. Chem, 1949, 80, 251-255.
[22] Kratky, O.; Porod, G. Recl. Röntgenuntersuchung gelöster Fadenmoleküle. Trav. Chim. 1949, 68, 1106-1122.

10. ACRONYMS

AFM: Atomic Force Microscope
CR: Charge Regulation
DH: Debye Hückel
FJC: Freely Jointed Chain
GCMC: Grand Canonical Monte Carlo
HA: Hyaluronic Acid
LR: Long Range
MC: Monte Carlo
OLS: Optical Lever Sensitivity
PBS: Phosphate Buffered Saline
PE: Polyelectrolyte
SMFS: Single Molecule Force Spectroscopy
WLC: Wormlike Chain

APPENDICES

APPENDIX 1: CALIBRATION OF AFM CANTILEVER

The change in the position of the deflected laser beam on the photodiode reflects the bending or deflection of the AFM cantilever due to the interaction forces between the tip and the sample. In order to convert the photodiode signal into units of force, the spring constant of the cantilever (k_S) and the deflection sensitivity (S) of the detector must be calibrated before every measurement. The spring constant and invOLS calibration using the contact method is as follows. Note that the slope of the force-distance curve is the deflection sensitivity (S) or optical lever sensitivity (OLS), and its inverse is often referred to as invOLS.

1. Insert the cantilever into an AFM cantilever holder suitable for measuring in fluids.
2. Focus the laser beam at the very end of the cantilever where the tip is positioned and try to maximize the sum signal on the photodiode.
3. Adjust the position of the reflected beam to the middle of the segmented photodiode: zero vertical and horizontal deflection.
4. Put the surface into the AFM and cover it with a drop of liquid. Cantilever and surface should be now immersed in the liquid with the cantilever tip pointing toward the surface.
5. Acquire and save the thermal fluctuation spectrum of the cantilever. The cantilever must be sufficiently away from the surface, at least 50 μm, in order to exclude any surface damping effects. Usually, 10 or more spectra have to be accumulated to obtain a sufficient signal-to-noise ratio.
6. Approach the surface. In order to conserve tip geometry and tip functionalization the approach process has to be carried out carefully.
7. Determine invOLS ($nm.V^{-1}$) by pushing the cantilever tip against a hard surface. It is determined measuring the slope of the piezo travel distance against the change in the photodiode voltage. Fit a line to the part of the force distance curve where the cantilever tip is in contact with the surface. This parameter is necessary for the algorithm to determine the spring constant.
8. Finally, determine the spring constant ($pN.nm^{-1}$) by fitting a harmonic oscillator to the thermal noise spectrum.

APPENDIX 2: HISTOGRAMS OF DESORPTION FORCE

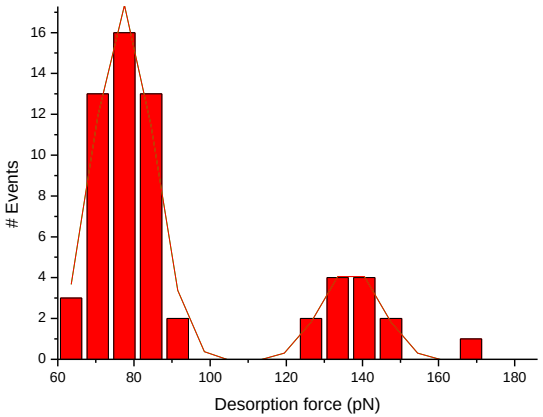

A.2.1. Histogram of desorption forces at pH 5.7 with glass surface

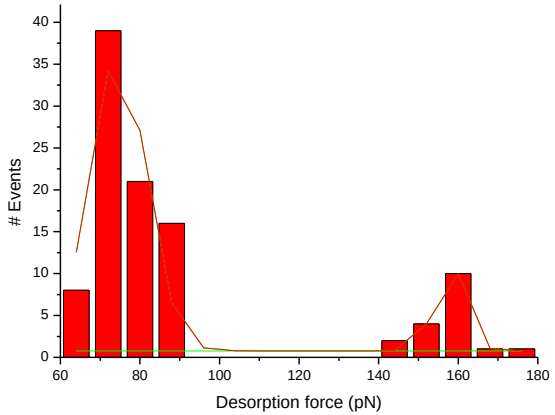

A.2.2. Histogram of desorption forces at pH 5.7 with silicon surface (cleaned with organic solvents)

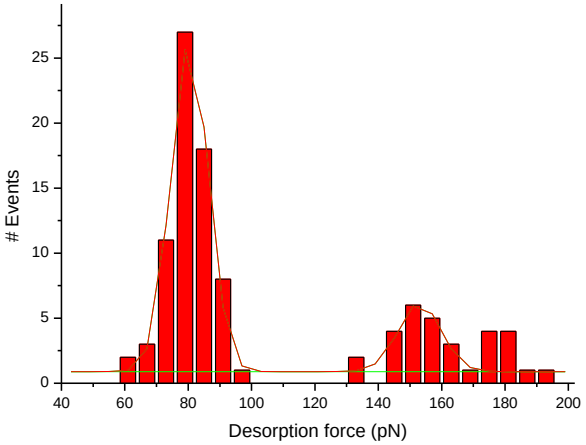

A.2.3. Histogram of desorption forces at pH 5.7 with silicon surface (cleaned with piranha)

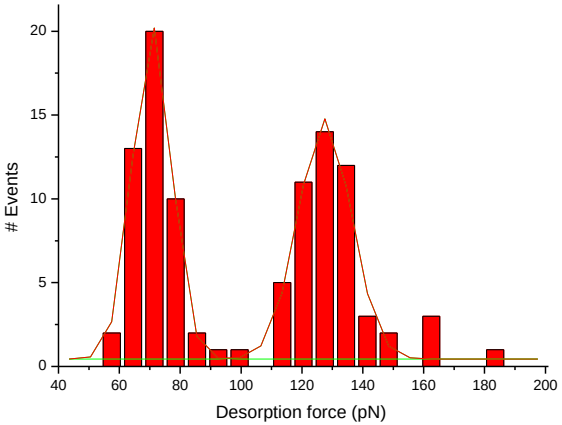

A.2.4. Histogram of desorption forces at pH 4 with silicon surface (cleaned with organic solvents)

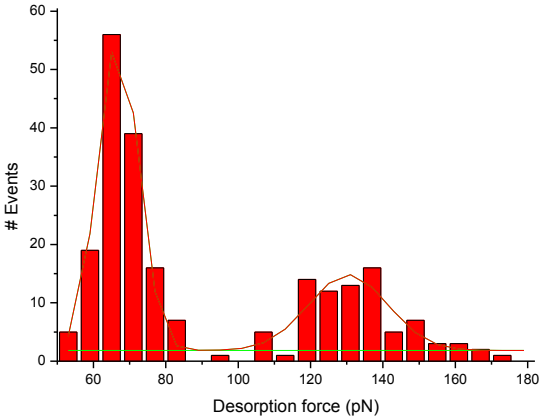

A.2.5. Histogram of desorption forces at pH 4 with silicon surface (cleaned with piranha)

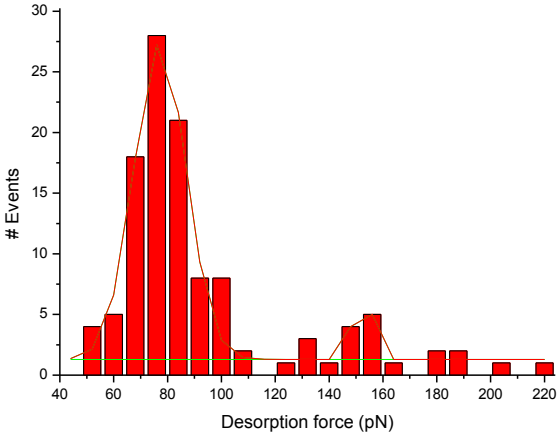

A.2.6. Histogram of desorption forces at pH 5.7 (0.1 M NaCl; cleaned with piranha)

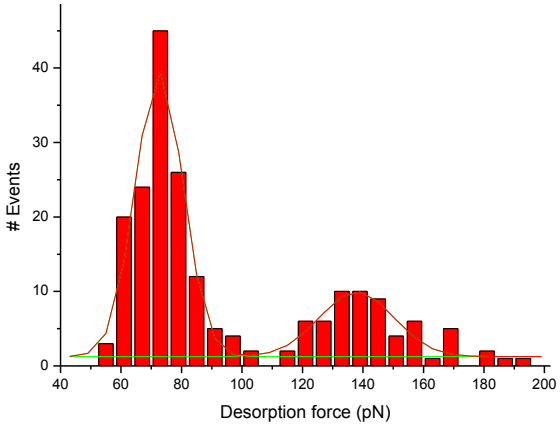

A.2.7. Histogram of desorption forces at pH 4 (0.1 M NaCl, cleaned with piranha)

APPENDIX 3: FORCE EXTENSION CURVES

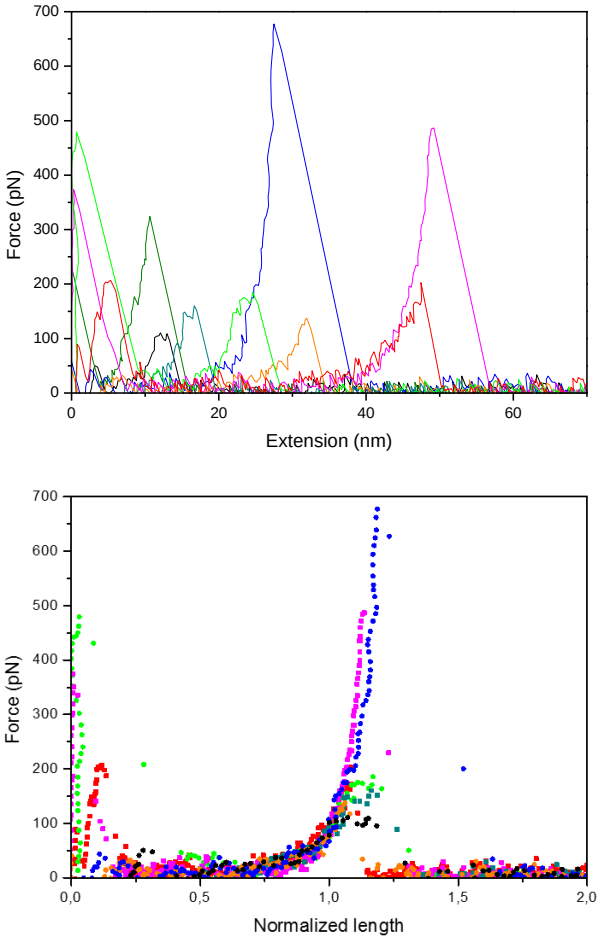

A.3.1 Force-extension traces of individual HA molecules measured at pH 5.7 and the corresponding normalization to a common force value of 100 pN.

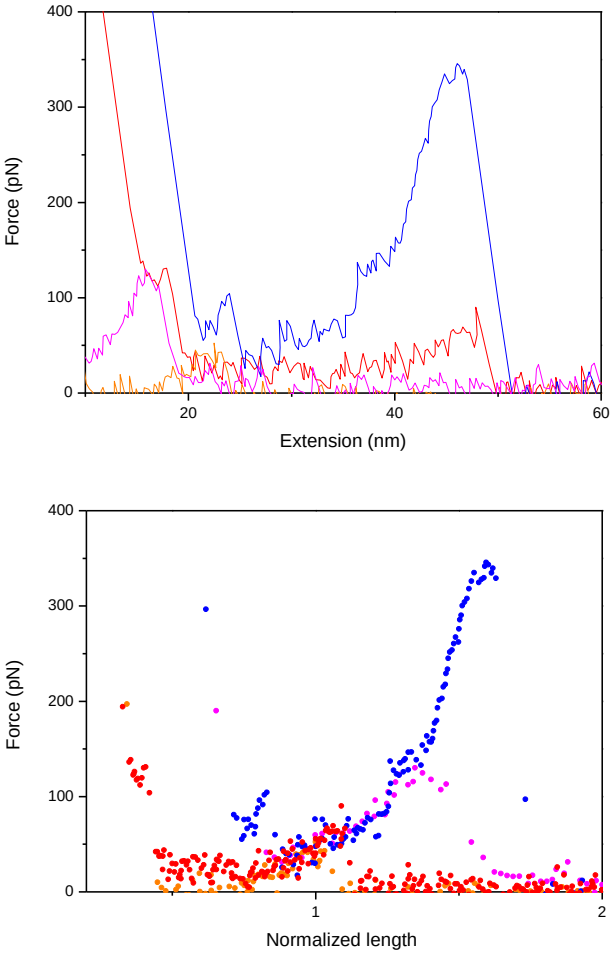

A.3.2. Force-extension traces of individual HA molecules measured at pH 4 and the corresponding normalization to a common force value of 50 pN.

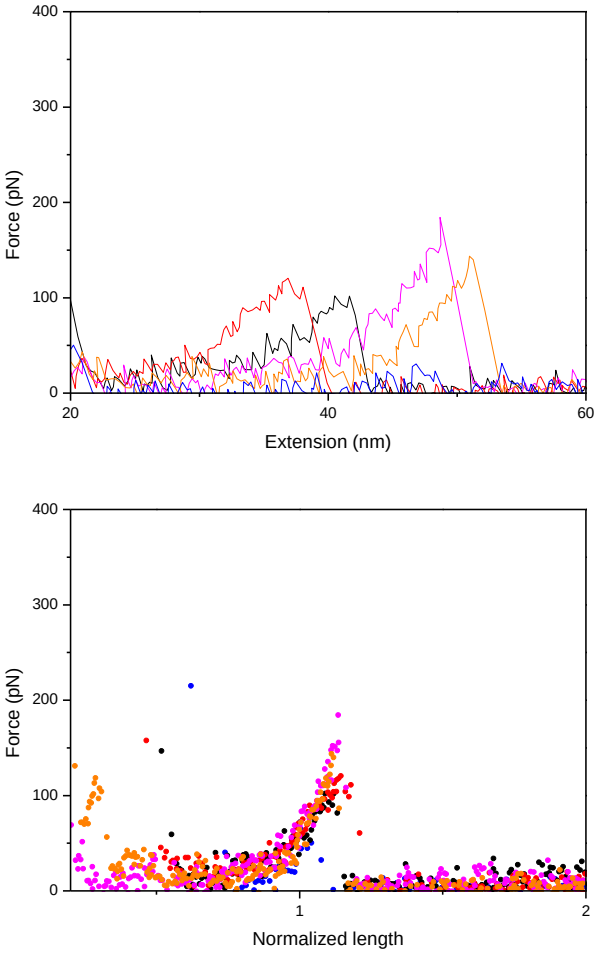

A.3.3. Force-extension traces of individual HA molecules measured at pH 5.7 in 0.1 M NaCl solution and the corresponding normalization to a common force value of 50 pN.